

Acoustic Properties of the Otolith of the Large Yellow Croaker *Larimichthys crocea* (Perciformes: Sciaenidae)

Xin-Hai Zhang¹ , Yi Tao^{1,*} , Yang-Liang Zhou¹ , Li-Guo Tang¹ , Min Liu² , and Xiao-Mei Xu¹ 

¹Key Laboratory of Underwater Acoustic Communication and Marine Information Technology of Ministry of Education, College of Ocean and Earth Sciences, Xiamen University, Xiamen, Fujian Province, China. *Correspondence: E-mail: taoyi@xmu.edu.cn (Tao). E-mail: xhzhang@stu.xmu.edu.cn (Zhang); zhouyangliang@stu.xmu.edu.cn (Zhou); liguotang@xmu.edu.cn (Tang); xmxu@xmu.edu.cn (Xu).

²Dongshan Swire Marine Station, College of Ocean and Earth Sciences, Xiamen University, Xiamen, Fujian Province, China. E-mail: minliuxm@xmu.edu.cn (Liu)

Received 11 March 2021 / Accepted 28 July 2021 / Published 3 November 2021
Communicated by Benny K.K. Chan

The inner ears of fish contain three pairs of otoliths—lapilli, asterisci and sagittae—which play important roles in hearing and balance. However, acoustic properties and dynamic responses of fish otoliths are poorly understood. The large yellow croaker (*Larimichthys crocea*), like many species in the family Sciaenidae, is extremely sensitive to sound. The present study used *L. crocea* sagittae as the research subject and examined the variation in shear stress on sagittae under different acoustic stimuli. For the first time, the sound speed of the sagitta was measured using ultrasonic pulse-echo techniques, and the acoustic impedance and natural frequency of the sagitta were calculated. *Larimichthys crocea* adults (20–22 cm standard length, $n = 10$) had a sagitta density of 2781.5 ± 28.06 kg/m³, sound speed of 4828–6000 m/s and acoustic impedance range of 13.4–16.7 MPa·s/m, approximately 9–11 times that of seawater (1.48 MPa·s/m). The natural frequency of the sagitta was 76.4–95.5 kHz. The shape and structural details of sagittae were reconstructed by 3D scanner and the shear stress responses of sagittae under different acoustic stimulus were investigated based on a finite element model. The simulation results showed that the shear stress responses tended to increase and then decrease in the range of sciaenid hearing frequency from 200 to 1300 Hz, peaking at 800 Hz. The shear stress responses varied with the direction of acoustic stimulus and peaked when the incident direction was perpendicular to the inner surface of the otolith. These results provide important parameters that may be used to protect *L. crocea* from possible underwater noise damage, particularly during their spawning aggregations and overwintering aggregations.

Key words: Sciaenidae, Otolith, Acoustic properties, Sound speed, Finite element modeling.

BACKGROUND

Underwater sound is critical to fish, as it helps them communication, detect predators and prey, navigate habitats (Tavolga 1971; Tolimieri et al. 2000; Simpson et al. 2005 2010; Ladich and Winkler 2017) and detect other long-range acoustic field information (Montgomery et al. 2006; Atema et al. 2015). Due to the low visibility

of the marine environment, the auditory organs in fishes are considered to be more important than visual organs (Popper and Hawkins 2018).

The inner ear of fish is an important auditory sensor; it includes three semicircular canals with paired otolith organs. A calcareous structure, consisting of about 90% calcium carbonate and minor amounts of organic materials, is present in each otolith organ

(Borelli et al. 2003). These dense otolith structures are categorized as lapilli, asterisci and sagittae, and are closely associated with the auditory sensory epithelium. The acoustic properties (density and elasticity) of fish tissue are very similar to the surrounding water. When the fish are exposed to sound, the otoliths function as an accelerometer. The otoliths are denser than the water and their motion lags relative to the water, thus creating a relative motion with the auditory hair cells (Krysl et al. 2012; Schulz-Mirbach et al. 2019). When hair cells are deflected by the relative movement, neurotransmitters are released into sensory epithelia to produce auditory responses (Fig. 1) (Flock 1971; Popper and Lu 2000).

The morphologies (shape and size) of otolith organs in the inner ear of fish are diverse, and this may affect the fish's hearing ability (Inoue et al. 2013; Kéver et al. 2014; YJ Lin et al. 2019; Schulz-Mirbach et al. 2019; Echreshavi et al. 2021). The clear differences in the size and shape of the otoliths suggest differences in their natural frequencies and responses to acoustic stimulus. The differences in fish auditory sensitivity caused by otolith morphology is apparent at the low frequency range. Large otoliths may be more sensitive to low frequency (Lychakov and Rebane 2000; Popper et al. 2005). An inverse relationship between otolith size and hearing range has been reported in previous literature, *i.e.*, the fish species with larger otoliths have a narrower hearing range (Lychakov and Rebane 2000; Finneran and Hastings 2000; Popper et al. 2005). For instance, hardhead catfish (*Ariopsis felis*) are more sensitive to low frequencies, and their upper hearing limit is low (< 900 Hz). On the contrary, other sea catfish species have hearing limits above 3000 Hz, but they are less sensitive to low frequencies than *A. felis*. This difference is because *A. felis* has particularly large lapilli, making it more sensitive to low frequencies (Popper and Tavolga 1981).

A very important marine fishery resource in China, the large yellow croaker (*Larimichthys crocea*, Sciaenidae), forms large spawning aggregations

in nearshore shallow waters and over-wintering aggregations in offshore deep waters (Liu and De Mitcheson 2008). *Larimichthys crocea* has large sagittae and is particularly sensitive to sound (Ramcharitar et al. 2006). In the 1950s and 1960s, the most common method for capturing *L. crocea* was luring them with a sound trap (Liu and De Mitcheson 2008). The morphological characteristics of *L. crocea* sagittae are: there is an umbo on the external surface, slightly convex on the inner (mesial) face with a tadpole-shaped impression (Lin and Chang 2012). Vocal behavior and sound sensitivity are features of sciaenid fish, and there have been some reports about their sound characteristics and how they are influenced by underwater noise. Japanese croakers (*Argyrosomus japonicus*) spawn accompanied by vocalization. Their sound is composed of pulse trains that are different between males and females (Ueng et al. 2007). The blackspotted croaker (*Protonibea diacanthus*) produces two sound types; the main type is composed of burst pulses with long intervals (Mok et al. 2009). The *L. crocea* produces sound while foraging and spawning, with a dominant frequency of about 800 Hz (Ren et al. 2007). Prolonged exposure to aquatic noise may cause chronic hazards to *L. crocea*, such as altered behavioral patterns and indirect mortality due to cumulative effects (Liu et al. 2014). When exposed to ship noise, *L. crocea* larvae show avoidance behavior, with concomitant increases in their blood cortisol, glucose, hemoglobin and lactic acid levels (TT Lin et al. 2019).

To better understand how the otolith contributes to hearing and balance, it is necessary to study and measure its acoustic properties. However, a lack of relevant data on this prevents us from understanding the specific roles of otolith in fish hearing. Previous studies have focused on the movement patterns of fish otoliths, and some studies have used mathematical models to represent fish otoliths as ellipsoids, suggesting that different otolith morphology may influence the fish's movements (Lychakov and Rebane 2000 2005; Krysl et

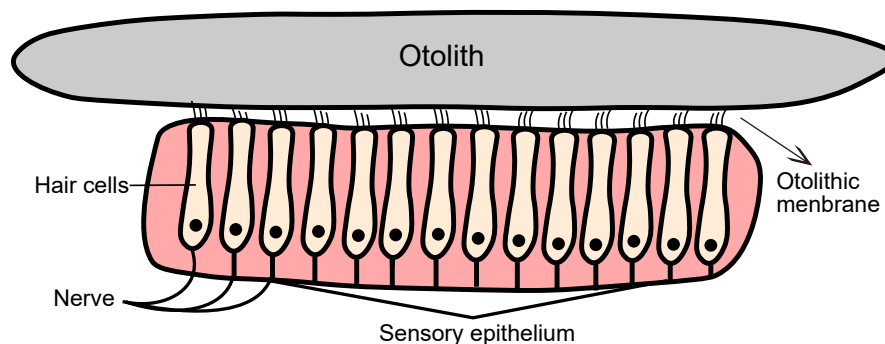


Fig. 1. Schematic diagram of the relationship between the sensory epithelium and the otolith.

al. 2012). The hypothesis around sound-induced otolith motion is mainly based on a mathematical model, and a visualization technique (X-ray phase contrast imaging) has recently been developed to visualize the sound-induced otolith movements (Schulz-Mirbach et al. 2018 2019). The above studies further illustrate the motion patterns of otoliths induced by sound, but unfortunately no one has focused on the acoustic properties of the otolith itself.

In this study, the sound speed of *L. crocea* sagitta was measured and calculated for the first time by the ultrasonic pulse-echo method. Using a 3D scanning technique and finite element modeling (FEM) to explore the acoustic responses and directionality of *L. crocea* sagittae. The results can provide an important reference for understanding the acoustic properties of the croaker and acoustical protection on croaker mariculture and spawning aggregation.

MATERIALS AND METHODS

Sound speed measurement

One of the most essential parameters for determining an object's acoustic properties is its sound speed. The acoustic impedance of an object and elastic modulus can be calculated by that object's sound speed and density. The ultrasonic pulse-echo method can quickly and accurately measure a sample's sound speed. The sound propagation has a good positive correlation with density, *i.e.*, the higher the density, the greater the sound speed.

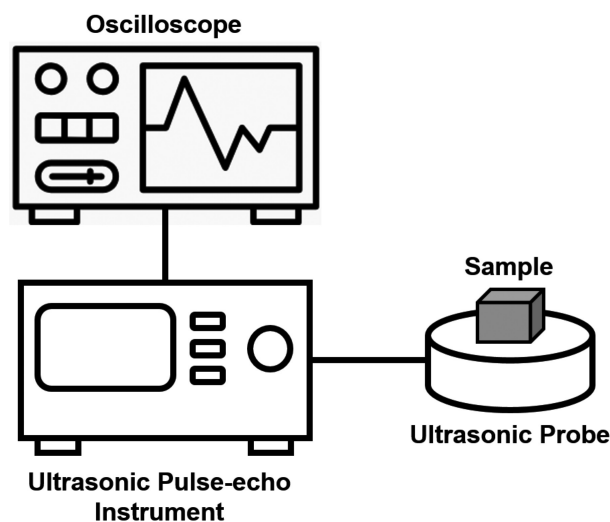


Fig. 2. Experimental setup for measuring the sound speed of *Larimichthys crocea* sagittae.

The ultrasonic pulse-echo method is mainly used to measure the difference in time (Δt) between two consecutive reflected waves in a sample, and use it to determine the sound speed (c) (equation 1). We used equation (2) to calculate the elastic modulus E , which reflects the elastic deformation capacity of the sample, where h is the sample thickness and ρ is the sample density.

$$c = \frac{2h}{\Delta t} \tag{1}$$

$$E = \rho c^2 \tag{2}$$

The measurement was performed by an ultrasonic pulse-echo instrument (CTS-8077PR, China, measuring probe frequency 10 MHz, pulse width 50 ns) (Fig. 2). The ultrasound method has reportedly been used to measure the acoustic properties of bone (Hakulinen et al. 2005; Riekkinen et al. 2007). The ultrasonic signal was evoked by a measurement transducer, and the pulse echoes were recorded by an oscilloscope (Tektronix MDO3024, USA). It is necessary to coat the surface of the probe with a coupling agent to ensure full contact between the sample and the ultrasonic probe. The sound speed of each sagitta was measured five times with the ultrasonic pulse echo method.

The acoustic impedance Z was calculated by equation (3), where ρ and c are the density and sound speed, respectively.

$$Z = \rho c \tag{3}$$

The natural frequency of an object depends on its stiffness and weight, the former of which is determined by the structure of the object. When an object is forced to vibrate, the vibration frequency depends on the frequency of the external force. When the external frequency is close to the natural frequency of the object, a significant vibration intensification will occur. The vibration frequency (or period) can be expressed by the simplified equation (4), where m is the weight of the object (kg), K is the stiffness coefficient (N/m) of the object, and T is the period (s). Based on the relationship between K and E ($K = E * A/L$), A and L represent the cross-sectional area and the length of the material, the equation (4) can be further expressed.

$$T = 2\pi \sqrt{\frac{m}{k}} = \frac{2\pi}{c} \sqrt{\frac{LV}{A}} \tag{4}$$

For a cube volume $V = A * L$, the natural frequency $f = 1/T$ can be estimated from the sound speed c and the length L by equation (5).

$$f = \frac{c}{2\pi L} \tag{5}$$

Treatment of sagittae

The paired sagittae were collected from 1-year-old cultured *L. crocea* ($n = 10$) fish with a standard length range (20–22 cm) (Fig. 3A). The cultured *L. crocea* were sampled from the Fufa aquaculture company (Fujian, China) on April 29, 2019. The sagittae were cut into cubes using a diamond wire cutting machine (STX-202A, China). The surfaces of the samples were polished using a precision grinding system (Unipul-802, China) (Fig. 3B). The thickness of the polished sample was measured by a digital dial indicator (ID-C125XB, Japan). The weight of each sagitta was measured by electronic balance (DS120-3, China) and the density was measured by an electronic densitometer (XF-120MD, China).

FEM for the acoustic response of the otoliths

The FEM simulation was used to predict the responses of *L. crocea* sagittae. The morphologies of the sagittae were reconstructed by 3D scanner with a measurement accuracy of 0.008 mm. The obtained morphological data were saved in the *.stl* file format. These morphological data (*.stl*) were imported into the software Comsol Multiphysics (v.5.4) to present and simulate their acoustic responses to different acoustic stimuli. The frequency of acoustic stimulus in our simulation was associated with the hearing abilities of sciaenid fish (Ramcharitar et al. 2006; Horodysky et al. 2008), set to 200–1300 Hz in steps of 100 Hz and a linear chirp type. In the Comsol software, the pressure acoustic transmission module combined with solid

mechanics and acoustic solid structure boundary module were applied to our FEM model. The spatial grid size controlled by the physical field, and the time step of the physical field was the reciprocal of the sampling frequency of 5000 Hz.

The model domain consisted of a fluid sphere zone with the acoustic properties of seawater (density 1000 kg/m^3 , sound speed 1480 m/s and acoustic impedance $1.48 \text{ MPa}\cdot\text{s/m}$). Since the fish body and seawater reportedly have very similar densities and acoustic properties (Popper and Hawkins 2018), this fluid sphere zone also represented the fish body and the environment surrounding the fish. A pair of sagittae was arranged according to its position in the fish ear (Fig. 4A), and were located in the center of the sphere. The sagittae were assumed to be isotropic, and the acoustic properties of our measurement results were used in this model. The sound source S was an incident plane wave and was rotated around the sagittae to analyze the response and the directionality of otoliths (Fig. 4B).

To improve the signal-to-noise ratio and eliminate inaccuracies in the FEM simulation results, the Teager-Kaiser energy operator (TKEO) method was used to analyze our simulation results. The idea behind TKEO is that its signal energy is not only amplitude dependent, but also related to the frequency (Kaiser 1990). The signal energy is not proportional to the amplitude square, but proportional to the amplitude and frequency product square. This idea has been accepted and is widely used in bio-signal processing (Li et al. 2007; Solnik et al. 2010).

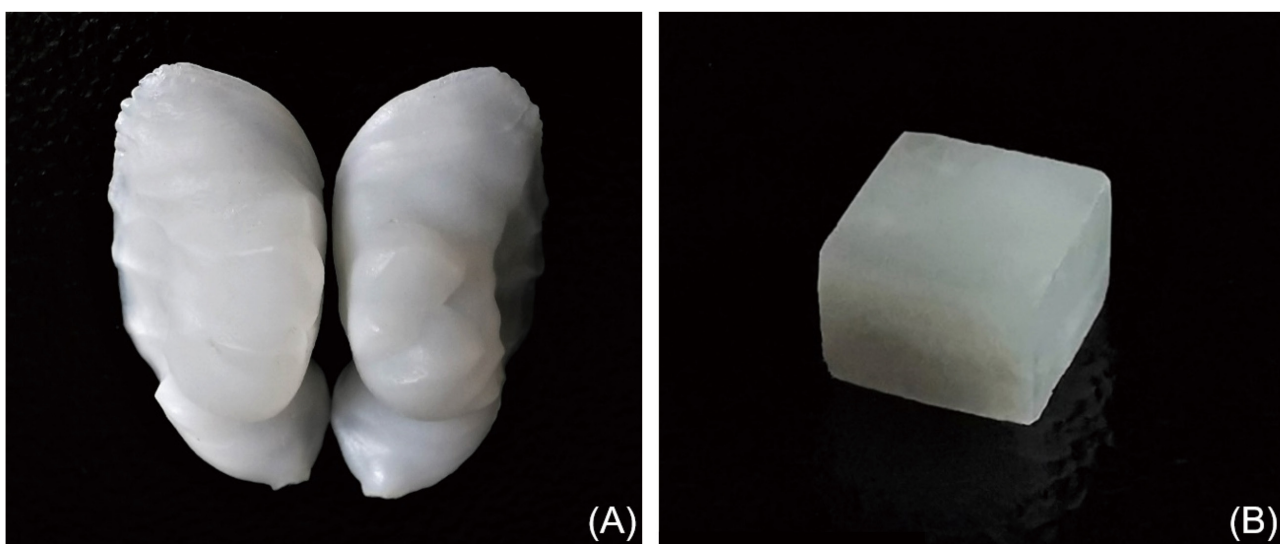


Fig. 3. (A) A pair of sagittae from *Larimichthys crocea*. (B) Polished sagitta sample.

RESULTS

Acoustic properties of sagittae

The typical pulse echo of the sagittae was recorded. The duration of the excitation signal was about 1 μs , and there was a clear echo after 1.5 μs (Fig. 5). The ultrasonic echo time difference (Δt) of the sagittae ranged from 0.8 to 1 μs . The sound speed of the sagittae ranged from 4828 to 6000 m/s, and the density was $2781.5 \pm 28.06 \text{ kg/m}^3$. The acoustic impedance of the sagittae was 13.4–16.7 MPa·s/m, approximately 9–11 times that of seawater (1.48 MPa·s/m). The length (L) of the sagittae was 0.01–0.015 m, and the sound speed (c) ranged from 4828 to 6000 m/s. The natural frequencies of sagittae were about 76.4 to 95.5 kHz.

Modeled acoustic response of the sagittae

The model simulated the shear stress responses of sagittae with different acoustic stimuli (400 and 800 Hz) from the same direction (Fig. 6). Shear stress responses represented the relative motion between the sagittae and the surrounding environment. The result suggested that the 800-Hz acoustic stimulus produced greater shear stress than the 400 Hz stimulus, especially in the inner surface of the sagittae. There was a relationship between shear stress response and frequency. With the frequency sweeps, the shear stress first increased, then showed a decreasing trend, peaking at 800 Hz (Fig. 7).

Changing the direction of the acoustic stimulus

may have altered the shear stress responses on the surface (Fig. 8). For a single sagitta, when the angle of incidence changed, the shear stress increased initially, then decreased, then increased again; the shear stress intensity was asymmetrical for each sagitta in the pair. The trend in sagittae shear stress responses was shaped like a butterfly. The normalized amplitude was highest at the 45° and 300° angles of incidence (in reference to the front of the sagittae), which is approximately perpendicular to the inner surface of the sagittae.

The relationship among shear stress responses and directionalities at different frequencies (400, 600, 800, 1000 and 1200 Hz) are shown in figure 9. The angle 0° represented the incident sound from the front, whereas -180° and +180° represented the left and right side of sagitta, respectively. The trends in shear stress and directionality at each frequency were similar for each sagitta. The strongest response occurred at 800 Hz, implying that *L. crocea* was sensitive to this frequency. Combining these results yielded polar contour plots (Fig. 10). The radius from the inside to the outside represented the frequency change, the corresponding frequency at the origin is 200 Hz, the outermost side corresponds to the frequency 1300 Hz. The color bar indicated the shear stress response intensity. The frequency responses of *L. crocea* sagittae were similar to an onion profile. There were two extreme points for each sagitta. This result demonstrated that the shear stress responses of *L. crocea* sagittae depended on the frequency and direction of the acoustic stimulus.

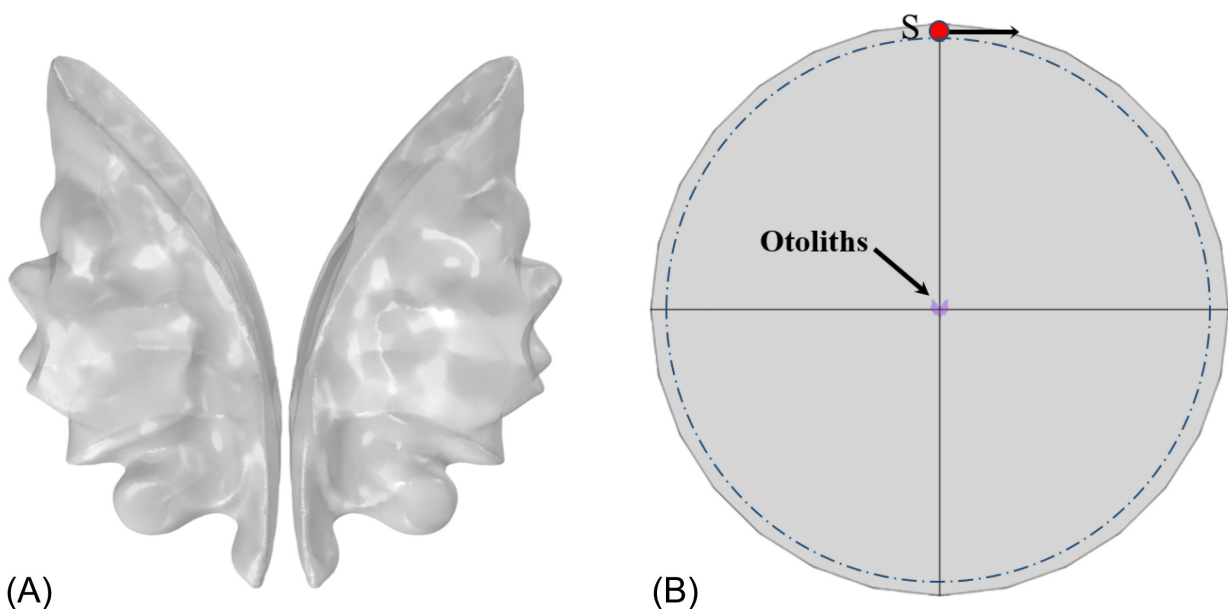


Fig. 4. (A) Reconstructed paired sagittae of *Larimichthys crocea* from a 3D scanner. (B) The layout of sagittae and sound source in the finite element model; the initial position of the sound source is in front of the sagittae.

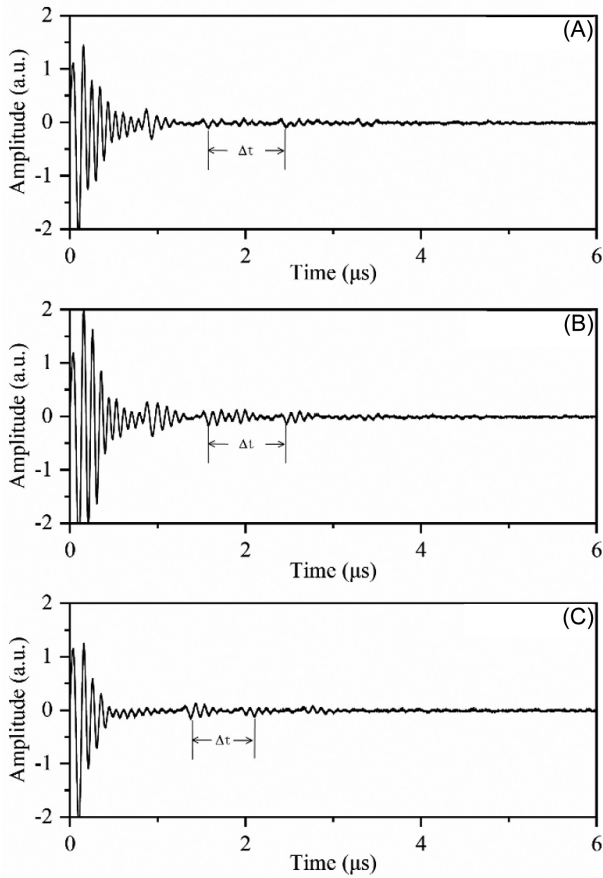


Fig. 5. The pulse echo measurement data from three sagittae of *Larimichthys crocea*. (A) sagitta 1; (B) sagitta 2; (C) sagitta 3.

DISCUSSION

In this study, the sound speed of *L. crocea* sagitta was successfully measured using the ultrasonic pulse-echo method for the first time. The results showed the sound speed to be between 4828 and 6000 m/s, and the acoustic impedance ranged from 13.4 to 16.7 MPa·s/m. The variation in sagitta shear stress was investigated by 3D scanning combined with a FEM approach, which helped us better understand the hearing mechanisms for *L. crocea*. According to our simulation results, the shear stress of sagittae is closely associated to the frequency of acoustic stimulus; it is also related to the hearing ability of *L. crocea*. Under different frequency stimulations, the shear stress of the sagittae varies. The shear stress response increased with increasing frequency, with the greatest response produced at 800 Hz acoustic stimulus (which is approximately five times that of the 200-Hz acoustic stimulation), and then decreased with increasing frequency. These results correspond to the distribution of the actual hearing capability of *L. crocea* in the frequency domain. Most sciaenid fish hear best at frequencies below 1000 Hz (Ladich and Fay 2013). Relevant literature on the hearing threshold of *L. crocea* indicated that the audible frequency of *L. crocea* is 100 to 4000 Hz and the most sensitive frequency is 500 to 800 Hz (Yin 2017). Additionally, one interesting result is that the sagittae responded slightly differently to symmetrical direction acoustic stimuli (e.g., Fig. 8 and Fig. 10). We speculated that this result may be

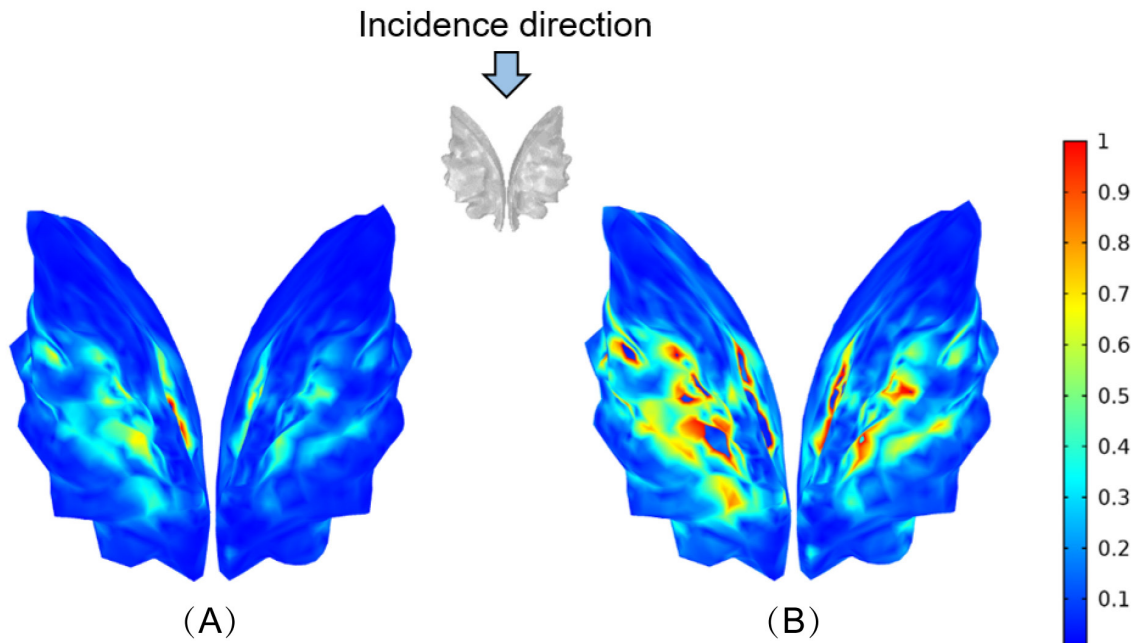


Fig. 6. The surface shear stress response of sagittae of *Larimichthys crocea* from sound signals at two frequencies: 400 Hz (A) and 800 Hz (B). Color variation indicates the magnitude of shear stress.

related to the external morphology of each sagitta, as there are minor differences in morphology details. The asymmetry in paired sagittae morphology has been reported in the red drum (*Sciaenops ocellatus*) and other fish species, such as the round goby (*Neogobius melanostomus*) and some roundfish and flatfish species (Browning et al. 2012; Mille et al. 2015; Więcaszek et al. 2020).

The potential hearing selectivity mechanism in fishes remains unclear, and there are gaps in our understanding of the effects and functions of otolith organs—*e.g.*, how interspecies hearing varies with different sagittae morphologies and sizes in fish (Fay et al. 1978; McKibben and Bass 2001; Weeg et al. 2002;

Ramcharitar and Popper 2004). Fish can respond to particle motion up to several hundred Hz through otolith organs, and the sagitta is considered to have specific auditory functions, like a particle motion receptor (Fay 1984; Fay and Simmons 1999; Schulz-Mirbach et al. 2019). Furthermore, fish can detect the location of the sound source. Some behavioral studies have reported that the fish inner ear is remarkably sensitive to sound from all directions (Lu et al. 1996). The selective auditory responses from various directions and the different directivity patterns of different otolith organs have been reported in several neurophysiological works (Fay 1984; Fay and Edds-Walton 1997; Lu et al. 1998; Popper and Hawkins 2018).

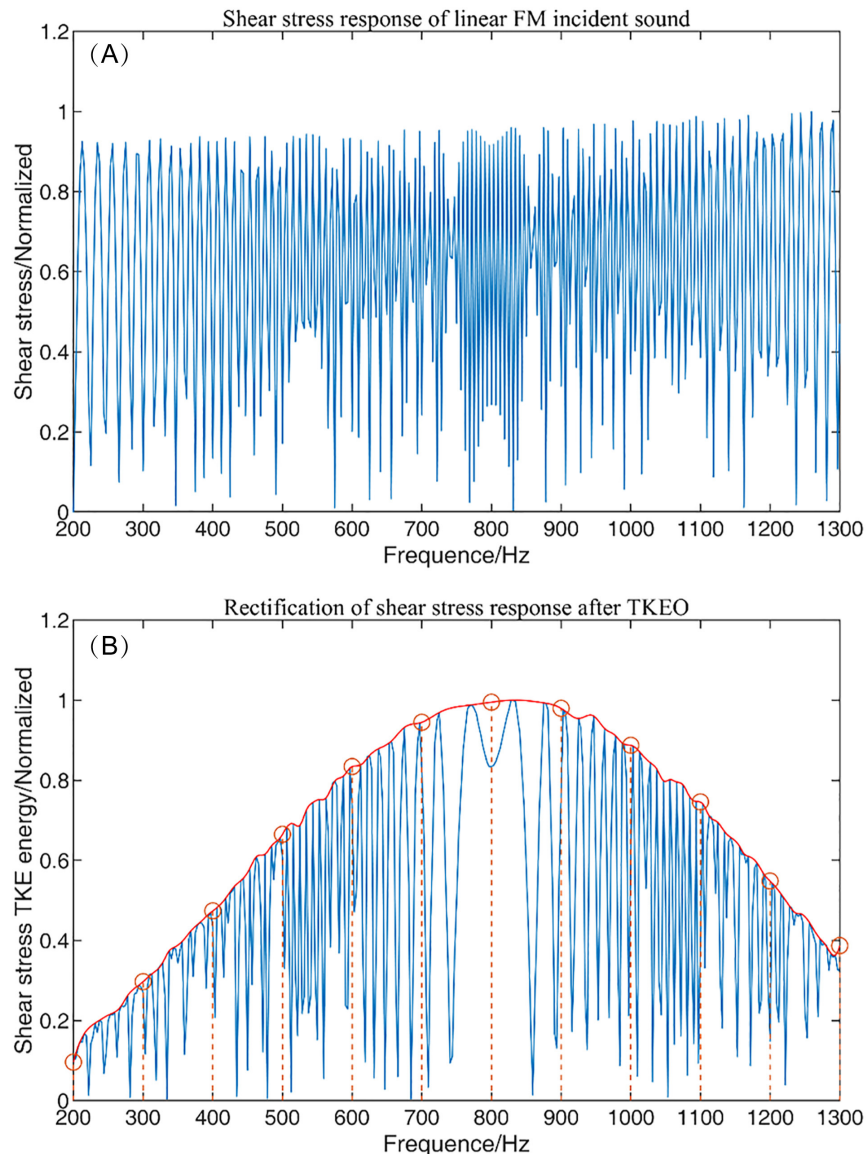


Fig. 7. Relationship between shear stress of sagittae (on the inner surface) and sound frequency; the incident angle of the sound wave is located in front of the sagittae. (A) Shear stress response of the sagittae; (B) shear stress response results after treatment with the TKEO method.

The results of our simulations also revealed that the sagittae of *L. crocea* can determine the orientation (or location) of the sound source. In our stimulation, changing the acoustic stimulus direction will result in a change in the shear stress responses on the sagittae, which produces varied responses. The shear stress response peaks when the incident acoustic wave is perpendicular to the inner surface of the sagittae. The

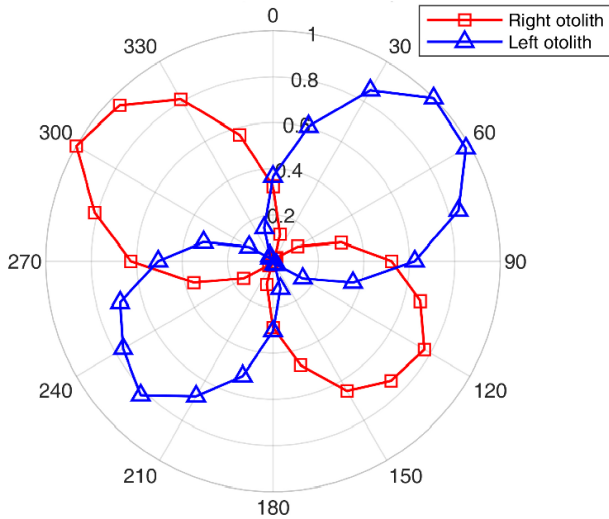


Fig. 8. Reception directivity of sagittae (exposed to 800 Hz sound wave) of *Larimichthys crocea*. The initial position of the sound source is at a 90° angle. Color corresponds to the left (blue) and right (red) sagitta.

results of these simulations illustrate that *L. crocea* may produce orientation ability because of the different shear stress produced by the sagittae to the sound in different directions. In addition, published literature indicated that the paired sagittae of the oyster toadfish (*Opsanus*

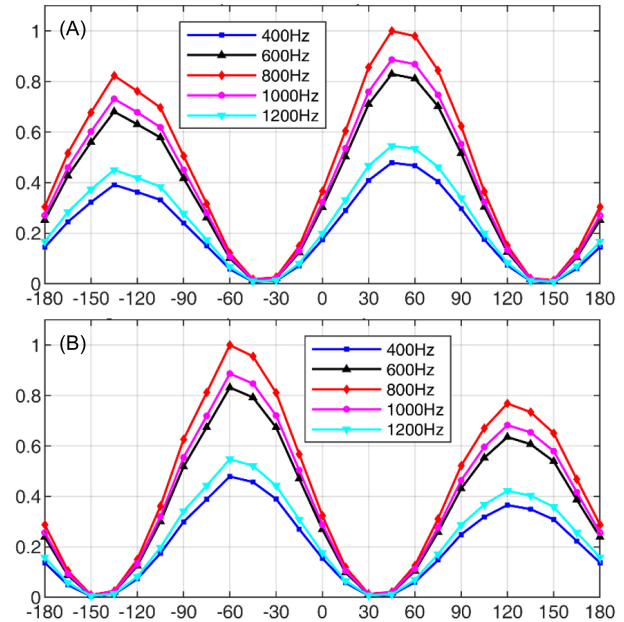


Fig. 9. The reception directivity and response intensity of each sagittae of *L. crocea* at different frequencies. (A) Left sagitta and (B) right sagitta. The x-axis represents the sound incidence angle; the y-axis represents the normalized response intensity. The incidence angle 0° represents the front of the sagittae, -180° represents the left side of the sagitta, and 180° represents the right side. Each color corresponds to a different sound frequency: 400 Hz (blue), 600 Hz (black), 800 Hz (red), 1000 Hz (purple), 1200 Hz (cyan).

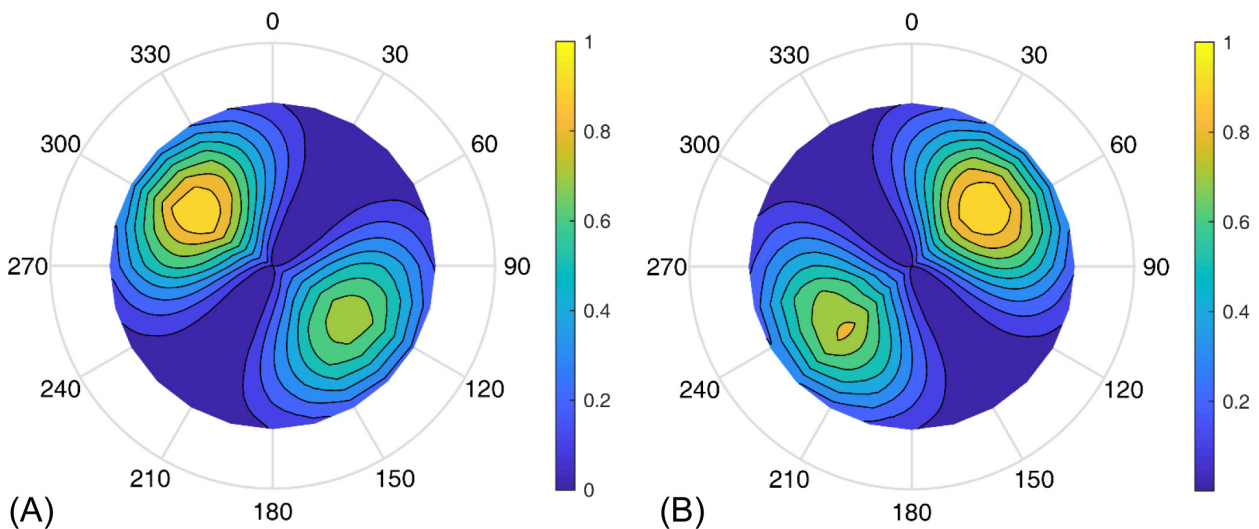


Fig. 10. The shear force response of the sagittae in the inner surface. (A) Left sagitta and (B) right sagitta. The initial position of the sound source is at 90°. Color variation indicates the magnitude of shear stress.

tau) can locate sound in various incident directions, and the sagittae will respond with different acoustic paths depending on the incident direction. Fish may use these acoustic path differences to estimate the direction of the sound source (Edds-Walton et al. 1999; Popper et al. 2003).

There are many intriguing questions about the otolith organ that may be explored with the FEM method. For instance, what is the relationship between the otolith organ and swimming bladder? Sciaenidae species are well known for generating a cacophony of knocking sounds, particularly when in spawning aggregations. During the reproductive period, *L. crocea* produces more sounds than usual; what is the major role of the otolith organ for hearing or for balance during this period? Furthermore, there is a considerable linear relationship between the fish length and sagitta radius of *L. crocea* larvae during the developmental stage (Liu et al. 2012). The method used in the present study can further explore changes in the hearing ability of *L. crocea* at different developmental stages. Noise also plays an important role in fish reproduction, especially during the hatching stage. The existing literature and experiments showed that the hatching rate of *L. crocea* eggs decreases in environments with loud noise (Meng et al. 2001). The acoustic FEM method used in this study can be used to further study the effect of noise intensity on the structure of *L. crocea* embryos. The main source of low-frequency ambient noise is the low-frequency radiation generated by ship operation, with a frequency of 5–1000 Hz (Urlick 1983). This frequency band is consistent with the acoustic sensitivity band of *L. crocea*, which covers the fish's vocal and auditory frequency, potentially masking their vocalization and hearing abilities. We can use the FEM method to evaluate how the underwater noises that ships produce may impact the growth and reproduction of *L. crocea*.

CONCLUSIONS

Sound is a key medium that fish use to perceive their marine environment. In the sensory system of fish, the inner ear is considered to be the most useful sensory receptor for obtaining and analyzing sound information. The otolith organs of the inner ear are implicated in hearing and balance functions. In this study, we used a unique ultrasonic pulse-echo method to preliminarily measure and calculate the acoustic properties of *L. crocea* sagittae. Using 3D scanning techniques and FEM methods, the shear stress responses of sagittae in an acoustic environment were simulated with different frequencies and directions. However, the methodology of this study may have some limitations or deficiencies.

On one hand, the functions of other smaller otolith organs (lapilli and asterisci) were not considered in the stimulation, but they may cooperate with the sagittae and further improve some hearing abilities of fish, e.g., frequency sensitivity and direction. On the other hand, the function of the swim bladder should be properly considered; the volume of the swim bladder changes slightly when sound fluctuates, leading the swim bladder to become a secondary sound source and re-radiate to the sagittae. Finally, whether the acoustic stimulus at a different intensity has an effect on the hearing function of the sagittae in *L. crocea* could also be further investigated in the future. The present simulation results provide fundamental data on sagittae acoustic properties and dynamic responses, which can improve future research on hearing in fish. The simulation results represent a simplified experimental scheme. The related structures such as cranial bones, other smaller otolith organs (lapilli and asterisci) and swim bladder should also be modeled and analyzed in future studies.

Acknowledgments: This work was supported by the National Key Research and Development Program of China (grant no. 2018YFC1406305), the National Nature Science Foundation of China (grant no. 41976178), and the Fujian Province Ocean and Fisheries Bureau of China (grant no. [3500] HTZB [GK] 2019007-1). We thank Li-Guo Tang for providing experimental equipment and technical guidance for the sound speed measurements. We are grateful to You-Gan Chen, Jian-Ming Wu, Xiao-Kang Zhang, Shen-Qin Huang and Wan-Wen Yan for providing experimental equipment and reviewing valuable comments on this manuscript.

Authors' contributions: XHZ designed the experiment. XHZ & YT wrote the first draft of this manuscript and performed data analyses. XHZ, YLZ & LGT conducted the experiment. XMX & ML revised the manuscript. All authors read and approved the final manuscript.

Competing interests: The authors declare that they have no competing interest.

Availability of data and materials: All the data and materials are provided within the manuscript.

Consent for publication: Not applicable.

Ethics approval consent to participate: Not applicable.

REFERENCES

- Atema J, Gerlach G, Paris CB. 2015. Sensory biology and navigation behavior of reef fish larvae. *In: Mora C (ed) Ecology of fishes on coral reefs*. Cambridge University Press, Cambridge, pp. 3–15. doi:10.1017/CBO9781316105412.003.
- Borelli G, Mayer-Gostan N, Merle PL, De Pontual H, Boeuf G, Allemand D, Payan P. 2003. Composition of biomineral organic matrices with special emphasis on turbot (*Psetta maxima*) otolith and endolymph. *Calcif Tissue Int* **72(6)**:717–725. doi:10.1007/s00223-001-2115-6.
- Browning ZS, Wilkes AA, Moore EJ, Lancon TW, Clubb FJ. 2012. The effect of otolith malformation on behavior and cortisol levels in juvenile red drum fish (*Sciaenops ocellatus*). *Comp Med* **62(4)**:251–256.
- Echreshavi S, Esmaili HR, Teimori A, Safaie M. 2021. Otolith morphology: a hidden tool in the taxonomic study of goatfishes (Teleostei: Perciformes: Mullidae). *Zool Stud* **60**:36. doi:10.6620/ZS.2021.60-36.
- Edds-Walton PL, Fay RR, Highstein SM. 1999. Dendritic arbors and central projections of physiologically characterized auditory fibers from the sacculle of the toadfish, *Opsanus tau*. *J Comp Neurol* **411(2)**:212–238.
- Fay RR. 1984. The goldfish ear codes the axis of acoustic particle motion in three dimensions. *Science* **225(4665)**:951–954. doi:10.1126/science.6474161.
- Fay RR, Ahroon WA, Orawski AA. 1978. Auditory masking patterns in the goldfish (*Carassius auratus*): psychophysical tuning curves. *J Exp Biol* **74(1)**:83–100.
- Fay RR, Edds-Walton PL. 1997. Directional response properties of saccular afferents of the toadfish, *Opsanus tau*. *Hear Res* **111(1-2)**:1–21. doi:10.1016/s0378-5955(97)00083-x.
- Fay RR, Simmons AM. 1999. The sense of hearing in fishes and amphibians. *In: Fay RR, Popper AN (eds) Comparative hearing: fish and amphibians*. Springer Handbook of Auditory Research, vol 11. Springer, New York, pp. 269–318. doi:10.1007/978-1-4612-0533-3_7.
- Finneran JJ, Hastings MC. 2000. A mathematical analysis of the peripheral auditory system mechanics in the goldfish (*Carassius auratus*). *J Acoust Soc Am* **108(3)**:1308–1321. doi:10.1121/1.1286099.
- Flock Å. 1971. Sensory transduction in hair cells. *In: Loewenstein WR (ed) Principles of receptor physiology*. Handbook of Sensory Physiology, vol 1. Springer, Berlin, pp. 396–441. doi:10.1007/978-3-642-65063-5_14.
- Hakulinen MA, Day JS, Töyräs J, Timonen M, Kröger H, Weinans H, Kiviranta I, Jurvelin JS. 2005. Prediction of density and mechanical properties of human trabecular bone *in vitro* using ultrasound transmission and backscattering measurements at 0.2–6.7 MHz frequency range. *Phys Med Biol* **50(8)**:1629–1642. doi:10.1088/0031-9155/50/8/001.
- Horodysky AZ, Brill RW, Fine ML, Musick JA, Latour RJ. 2008. Acoustic pressure and particle motion thresholds in six sciaenid fishes. *J Exp Biol* **211(9)**:1504–1511. doi:10.1242/jeb.016196.
- Inoue M, Tanimoto M, Oda Y. 2013. The role of ear stone size in hair cell acoustic sensory transduction. *Sci Rep* **3**:2114. doi:10.1038/srep02114.
- Kaiser JF. 1990. On a simple algorithm to calculate the ‘energy’ of a signal. *In: International conference on acoustics, speech, and signal processing*, Albuquerque, NM, USA, 3-6 April 1990. doi:10.1109/ICASSP.1990.115702.
- Kéver L, Colleye O, Herrel A, Romans P, Parmentier E. 2014. Hearing capacities and otolith size in two ophidiiform species (*Ophidion rochei* and *Carapus acus*). *J Exp Biol* **217(14)**:2517–2525. doi:10.1242/jeb.105254.
- Krysl P, Hawkins AD, Schilt C, Cranford TW. 2012. Angular oscillation of solid scatterers in response to progressive planar acoustic waves: do fish otoliths rock? *PLoS ONE* **7(8)**:e42591. doi:10.1371/journal.pone.0042591.
- Ladich F, Fay RR. 2013. Auditory evoked potential audiometry in fish. *Rev Fish Biol Fish* **23(3)**:317–364. doi:10.1007/s11160-012-9297-z.
- Ladich F, Winkler H. 2017. Acoustic communication in terrestrial and aquatic vertebrates. *J Exp Biol* **220(13)**:2306–2317. doi:10.1242/jeb.132944.
- Li X, Zhou P, Aruin AS. 2007. Teager-Kaiser energy operation of surface EMG improves muscle activity onset detection. *Ann Biomed Eng* **35(9)**:1532–1538. doi:10.1007/s10439-007-9320-z.
- Lin CH, Chang CW. 2012. Otolith atlas of Taiwan fishes. National Museum of Marine Biology and Aquarium.
- Lin TT, Wang CB, Liu X, Zhang D. 2019. Impacts of ship noise on the growth and immunophysiological response in the juveniles of two Sciaenidae species, *Larimichthys crocea* and *Nibea albiflora*. *J Appl Ichthyol* **35(6)**:1234–1241. doi:10.1111/jai.13976.
- Lin YJ, Qurban MA, Shen KN, Chao NL. 2019. Delimitation of tigertooth croaker *Otolithes* species (Teleostei: Sciaenidae) from the western Arabian Gulf using an integrative approach, with a description of *Otolithes arabicus* sp. nov. *Zool Stud* **58**:10. doi:10.6620/ZS.2019.58-10.
- Liu M, De Mitcheson YS. 2008. Profile of a fishery collapse: why mariculture failed to save the large yellow croaker. *Fish Fish* **9(3)**:219–242. doi:10.1111/j.1467-2979.2008.00278.x.
- Liu ZW, Xu XM, Huang EH, Yang YM. 2014. Study on behavior of sound stimulation for large yellow croaker (*Pseudosciaena crocea*). *J Appl Oceanogr China* **33**:105–110. (in Chinese)
- Liu ZY, Li SF, Xu XM, Zhang Y, Li YX. 2012. Morphological development and microstructure of sagittal otolith of large yellow croaker, *Larimichthys crocea* during larval and early juvenile stages. *J Fish Sci China* **19(5)**:863–871. (in Chinese)
- Lu Z, Popper AN, Fay RR. 1996. Behavioral detection of acoustic particle motion by a teleost fish (*Astronotus ocellatus*): sensitivity and directionality. *J Comp Physiol A* **179(2)**:227–233. doi:10.1007/BF00222789.
- Lu Z, Song J, Popper AN. 1998. Encoding of acoustic directional information by saccular afferents of the sleeper goby, *Dormitator latifrons*. *J Comp Physiol A* **182(6)**:805–815. doi:10.1007/s003590050225.
- Lychakov DV, Rebane YT. 2000. Otolith regularities. *Hear Res* **143(1-2)**:83–102. doi:10.1016/s0378-5955(00)00026-5.
- Lychakov DV, Rebane YT. 2005. Fish otolith mass asymmetry: morphometry and influence on acoustic functionality. *Hear Res* **201(1-2)**:55–69. doi:10.1016/j.heares.2004.08.017.
- McKibben JR, Bass AH. 2001. Peripheral encoding of behaviorally relevant acoustic signals in a vocal fish: harmonic and beat stimuli. *J Comp Physiol A* **187(4)**:271–285. doi:10.1007/s003590100199.
- Meng ZN, Hong WS, Wang QC, Zhang YQ, Bian HL. 2001. Study on the effects of ultrasonic wave on hatching of fertilized egg in four marine fishes. *Journal of Xiamen University Natural Science* **40(3)**:834–834. (in Chinese)
- Mille T, Mahe K, Villanueva MC, De Pontual H, Ernande B. 2015. Sagittal otolith morphogenesis asymmetry in marine fishes. *J Fish Biol* **87(3)**:646–663. doi:10.1111/jfb.12746.
- Mok HK, Yu HY, Ueng JP, Wei RC. 2009. Characterization of sounds of the blackspotted croaker *Protonibea diacanthus* (Sciaenidae) and localization of its spawning sites in estuarine coastal waters of Taiwan. *Zool Stud* **48(3)**:325–333.
- Montgomery JC, Jeffs A, Simpson SD, Meekan M, Tindle C. 2006. Sound as an orientation cue for the pelagic larvae of reef

- fishes and decapod crustaceans. *Adv Mar Biol* **51**:143–196. doi:10.1016/S0065-2881(06)51003-X.
- Popper AN, Fay RR, Platt C, Sand O. 2003. Sound Detection Mechanisms and Capabilities of Teleost Fishes. *In*: Collin SP, Marshall NJ (eds) *Sensory processing in aquatic environments*. Springer, New York, pp. 3–38. doi:10.1007/978-0-387-22628-6_1.
- Popper AN, Hawkins AD. 2018. The importance of particle motion to fishes and invertebrates. *J Acoust Soc Am* **143**(1):470–488. doi:10.1121/1.5021594.
- Popper AN, Lu Z. 2000. Structure-function relationships in fish otolith organs. *Fish Res* **46**(1-3):15–25. doi:10.1016/S0165-7836(00)00129-6.
- Popper AN, Ramcharitar J, Campana SE. 2005. Why otoliths? Insights from inner ear physiology and fisheries biology. *Mar Freshwater Res* **56**(5):497–504. doi:10.1071/MF04267.
- Popper AN, Tavolga WN. 1981. Structure and function of the ear in the marine catfish, *Arius felis*. *J Comp Physiol A* **144**(1):27–34. doi:10.1007/BF00612794.
- Ramcharitar J, Gannon DP, Popper AN. 2006. Bioacoustics of fishes of the family Sciaenidae (croakers and drums). *T Am Fish Soc* **135**(5):1409–1431. doi:10.1577/T05-207.1.
- Ramcharitar J, Popper AN. 2004. Masked auditory thresholds in sciaenid fishes: a comparative study. *J Acoust Soc Am* **116**(3):1687–1691. doi:10.1121/1.1771614.
- Ren XM, Gao DZ, Yao YL, Yang F, Liu JF, Xie FJ. 2007. Occurrence and characteristic of sound in large yellow croaker (*Pseudosciaena crocea*). *Journal of Dalian Fisheries University* **22**(2):123–128. (in Chinese)
- Riekkinen O, Hakulinen MA, Lammi MJ, Jurvelin JS, Kallioniemi A, Töyräs J. 2007. Acoustic properties of trabecular bone—relationships to tissue composition. *Ultrasound Med Biol* **33**(9):1438–1444. doi:10.1016/j.ultrasmedbio.2007.04.004.
- Schulz-Mirbach T, Ladich F, Plath M, Heß M. 2019. Enigmatic ear stones: what we know about the functional role and evolution of fish otoliths. *Biol Rev Camb Philos Soc* **94**(2):457–482. doi:10.1111/brv.12463.
- Schulz-Mirbach T, Olbinado M, Rack A, Mittone A, Bravin A, Melzer RR, Ladich F, Heß M. 2018. *In-situ* visualization of sound-induced otolith motion using hard X-ray phase contrast imaging. *Sci Rep* **8**(1):3121. doi:10.1038/s41598-018-21367-0.
- Simpson SD, Meekan M, Montgomery J, McCauley R, Jeffs A. 2005. Homeward sound. *Science* **308**(5719):221. doi:10.1126/science.1107406.
- Simpson SD, Meekan MG, Larsen NJ, McCauley RD, Jeffs A. 2010. Behavioral plasticity in larval reef fish: orientation is influenced by recent acoustic experiences. *Behav Ecol* **21**(5):1098–1105. doi:10.1093/beheco/arq117.
- Solnik S, Rider P, Steinweg K, DeVita P, Hortobágyi T. 2010. Teager-Kaiser energy operator signal conditioning improves EMG onset detection. *Eur J Appl Physiol* **110**(3):489–498. doi:10.1007/s00421-010-1521-8.
- Tavolga WN. 1971. Sound production and detection. *In*: Hoar WS, Randall DJ (eds) *Fish physiology*, vol 5. Academic Press, New York, pp. 135–205.
- Tolimieri N, Jeffs A, Montgomery JC. 2000. Ambient sound as a cue for navigation by the pelagic larvae of reef fishes. *Mar Ecol Prog Ser* **207**:219–224. doi:10.3354/meps207219.
- Ueng JP, Huang BQ, Mok HK. 2007. Sexual differences in the spawning sounds of Japanese croaker, *Argyrosomus japonicus* (Sciaenidae). *Zool Stud* **46**(1):103–110.
- Urick RJ. 1983. *Principles of underwater sound*. McGraw-Hill, New York, USA.
- Weeg MS, Fay RR, Bass AH. 2002. Directionality and frequency tuning of primary saccular afferents of a vocal fish, the plainfin midshipman (*Porichthys notatus*). *J Comp Physiol A* **188**(8):631–641. doi:10.1007/s00359-002-0338-2.
- Więcaszek B, Nowosielski A, Dąbrowski J, Górecka K, Keszka S, Strzelczak A. 2020. Fish size effect on sagittal otolith outer shape variability in round goby *Neogobius melanostomus* (Pallas 1814). *J Fish Biol* **97**(5):1520–1541. doi:10.1111/jfb.14521.
- Yin LM. 2017. The behavior response and attractive mechanism of *Larimichthys crocea* to acoustic stimulus. PhD dissertation, Shanghai Ocean University, China.